Rheological Characterization of Flow and Crystallization Behavior of Microbial Synthesized Poly(3-hydroxybutyrate-*co*-4-hydroxybutyrate)

Zhiyong Zhu, Piwai Dakwa, Prashant Tapadia, Robert S. Whitehouse,† and Shi-Qing Wang*

Department of Polymer Science, The University of Akron, Akron, Ohio 44325-3909

Received February 20, 2003; Revised Manuscript Received May 1, 2003

ABSTRACT: Rheological properties of a series of microbially synthesized poly(3-hydroxybutyrate-*co*-4-hydroxybutyrate)s, P(3HB-*co*-4HB)s, with different molecular weights and 4HB compositions have been systematically investigated. Capillary and oscillatory shear measurements have been carried out to characterize the flow behavior of these biopolyesters as a function of temperature at different flow conditions. The rheological characteristics of these samples show that the 4HB content does not appear to strongly affect the critical molecular weight M_e for chain entanglement. Under low stresses during creep measurements, the shear viscosity of a sample with low 4HB content diverges abruptly in a narrow temperature range due to the polymer crystallization. The same sample can still undergo capillary flow below the melting temperature at high stresses where the sample yields. Apart from the creep measurements, the crystallization behavior of the semicrystalline sample has been further characterized using stress-controlled oscillatory shear measurements during a cooling−heating cycle at a constant rate of temperature ramping. The rapid increase and decrease of the dynamic viscosity and storage modulus are interpreted as corresponding to crystallization and melting, respectively, during the thermal cycle. These rheologically determined crystallization and melting temperatures have been found to be ca. 20 °C apart and over 30 °C higher than those indicated by the DSC measurement.

Introduction

Biosynthesized poly(hydroxyalkanoate)s, (PHA)s, have attracted lots of attention in recent years as a potential candidate to substitute conventional thermoplastics such as polypropylene (PP) and polyethylene (PE), since they are biodegradable, biocompatible, and renewable. To compensate for the fragility of pure PHA materials, copolymers of PHAs like poly(3-hydroxybutyrate-*co*-4-hydroxybutyrate), P(3HB-*co*-4HB), and poly(3-hydroxybutyrate-*co*-3-hydroxyvalerate), P(3HA-*co*-3HV), are more often considered, and the composition variation may result in a wide range of potential applications from rigid thermoplastics to elastic rubber materials.[1] Synthesized by *Alcaligenes latus*,[2] *Ralstonia eutropha*,[3] or *Comamonas acidovorans*[4] in nitrogen-limited cultures containing 4-hydroxybutyric acid, γ-butyrolactone, 1,4-butandiol, 1,6-hexanediol, 4-chlorobutyric acid, or their blends as carbon sources, or directly chemically synthesized at a higher cost,[5] a wide range of P(3HB-*co*-4HB) copolymers with 4HB compositions from 0 to 100% can be made. One of these copolymers has also been commercially available from ICI with the brand name of Biopol through *A. eutrophus* by feeding propionic acid and glucose as carbon sources.

The application of PHAs and their copolymers depends on understanding of their processing behavior. As semicrystalline polymers, pure PHAs have melting temperatures (T_m) very close to their thermal degradation limits around 180 °C.[1] Thus, copolymers like P(3HB-*co*-4HB) are also used to adjust the material crystallization level and make the processing possible. The crystallization and thermal degradation behavior of P(3HB-*co*-4HB)s have been widely investigated.[6−11] These studies show that the 4HB units act as crystal defects in the copolymer, and with increasing 4HB both the crystallization level and the crystallization rate decrease; T_m of such copolymers can vary between 180 and 100 °C depending on the 4HB content. There is little crystallization when the 4HB content increases to above 25%.[1] The thermal degradation of P(3HB-*co*-4HB) is found to occur usually at temperature higher than 180 °C through a six-member-ring ester decomposition process. There is little degradation below 170 °C within 20 min.[1] Thus, for any P(3HB-*co*-4HB) copolymer with a melting point lower than 160−150 °C, a melt processing is feasible. The glass transition temperature T_g of P(3HB-*co*-4HB) copolymers is also found to decrease with the increasing content of 4HB.[12] The ^{13}C nuclear magnetic relaxation spectrum also shows the existence of 4HB hastens the segmental motions for both 3HB units and 4HB units compared with their bulk polymers.[13,14]

Despite their relevance to processing, rheological properties of biosynthesized PHAs and their copolymers have seldom been reported. Choi and co-workers[15,16] reported the rheological characterization of P(3HB-*co*-3HV)s with up to 20% 3HV and compared the oscillatory shear data and capillary flow data in a modified Cole−Cole plot. They also characterized PHB/PEO blends in a similar way.[17] The purpose of this paper is to carry out an extensive rheological characterization of a series of microbial synthesized P(3HB-*co*-4HB)s of different molecular weights and compositions (up to 37% 4HB) and to report the first rheological characterization of the polymers using capillary flow, creep, and stress controlled oscillatory shear measurements. By following the rheological change of the semicrystalline P(3HB-*co*-4HB) samples, we have been able to evaluate the crystallization process in situ and to reveal a correlation between crystallization and rheological properties. Exploring such interplay between the crystallization be-

† Metabolix Inc., Cambridge, MA 02142-1126.
* Corresponding author. E-mail: swang@uakron.edu.

10.1021/ma034219k CCC: $25.00
Published on Web 06/07/2003

Table 1. Characterization of P(3HB-*co*-4HB) Biopolyester Samples

sample	M_w ($\times 10^{-3}$)	M_n ($\times 10^{-3}$)	MWD	% 4PHB
A	133	69.7	1.9	14
B	412	191	2.2	20
C	196	105	1.9	27
D	386	178	2.2	31
E	1022	393	2.6	35
F	185	76.6	2.36	11
G	218	96.7	2.25	11
H	228	116	1.97	11
I	414	164	2.52	11
J	878	503	1.75	11

havior and rheological characteristics will not only provide an important guide in the choice of these biopolyesters for application and in processing design but will also lead to a general methodology applicable to all traditional semicrystalline polymers.

Experimental Section

Materials. The polyester copolymers poly(3-hydroxybutyrate-*co*-4-hydroxybutyrate) (3PHB-*co*-4PHB) used in this work were synthesized by Metabolix Inc. through *A. latus* in nitrogen-limited cultures with 4-hydroxybutyric acid fed as carbonic sources. The molecular weights, molecular weight distributions, and mole ratios of 4HB of these samples were characterized with GPC and NMR in Metabolix Inc. as listed in Table 1. The samples are labeled from A to E according to their 4HB content from low to high and from F to J according to their molecular weights. All the samples are in the powder form and were vacuumed for at least 48 h to remove moisture before usage.

Apparatus. A pressure-controlled Monsanto automatic capillary rheometer (MACR) was employed to measure the steady flow properties of P(3HB-*co*-4HB) copolymers using an aluminum capillary die of diameter $D = 1.12$ mm and length-to-diameter ratio $L/D = 20$ and an entry angle of 60°. A nitrogen tank generates the pressure P on the piston in the barrel, and the apparent shear stress on the wall is computed according to $\sigma = (D/4L)P$ without the Bagley entry effect correction. The apparent shear rate on the wall is calculated according to $\dot{\gamma} = 32Q/\pi D^3$ without the Rabinowitsch correction, in which the flow rate Q is obtained by collecting and weighing the extrudate: $Q = W/\rho t$, where W is the weight of the extrudate, ρ is the density of the extrudate (0.9 g/cm^3), and t is the time for such extrudate to flow out of the die.

A strain-controlled dynamic mechanical spectrometer (ARES) was applied to measure the viscoelastic properties of some of the PBD samples based on oscillatory shear. The ARES is equipped with a 200−2000 g·cm dual range force rebalance transducer, and oscillatory shear measurement was carried out using an 8 mm diameter parallel-plate flow cell at frequencies from 0.1 to 100 rad/s and temperatures from −20 to 160 °C. A stress-controlled dynamic mechanical spectrometer (Bohlin) was used to explore the creep behavior and the oscillatory shear response in a heating−cooling thermal cycle. The Bohlin is equipped with a pair of parallel plates of diameter $D = 15$ mm. The 1 mm thick disk samples for both ARES and Bohlin were prepared with a hot press at 150 °C for 10 min followed by cooling it to room temperature under a small level of pressure.

Differential scanning calorimetry (DSC) measurements were also performed on a TA DSC 2910 instrument to investigate the crystallization behavior of the biopolyesters. Samples (3−5 mg) held in aluminum pans were heated from room temperature to 160 °C at a rate of 10 °C/min (the first heating scan). We also carried out a heating−cooling experiment for sample A to compare the DSC response with the oscillatory shear response in a similar thermal cycle.

Results and Discussion

Melting Behavior by DSC. P(3HB-*co*-4HB) copolymers are typical semicrystallized polymers and therefore generally have a broad melting temperature range. The melting behavior of samples A to D is first characterized with DSC measurement in the first heating scan from 30 to 160 °C at a heating rate of 10 °C/min, as shown in Figure 1. Both sample A and sample B show two melting peaks in 50−60 and 90−100 °C, which are due to the 4HB-rich and 3HB-rich crystallization phases, respectively.[1,3] The peak area in 90−100 °C is much bigger than that in 50−60 °C, showing that the 3HB-rich phase comprises in the main part of the crystallization in the sample. It is noticed that sample B has melting temperature ~10 °C higher than that of sample A at both melting peaks. Sample C gives a very weak peak only at 58 °C, showing probably the existence of a very little amount of 4HB-rich crystallization region. There is no melting peak for sample D in the temperature range between 50 and 160 °C, indicating that it is essentially amorphous. This corroborates the earlier observation that the level of crystallinity diminishes with the increasing content of 4HB above 25%.

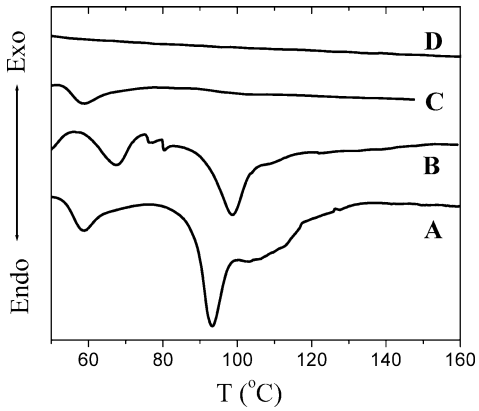

Figure 1. DSC thermograms for samples A−D during a heating scan from 30 to 160 °C at a heating rate of 10 °C/min.

Oscillatory Shear Measurement. To obtain linear viscoelastic characteristics of these biopolyesters, oscillatory shear measurements were first conducted with a strain-controlled dynamic mechanical spectrometer (ARES). Since sample D is essentially amorphous, the master curve can be obtained using time−temperature superposition (tTs). The disk-shaped sample of 1 mm thickness and 8 mm diameter was first loaded at 120 °C in order to ensure a good contact between the sample and the parallel plates, and then the oscillatory shear measurements were conducted from 160 to −20 °C in an interval of 20 °C. Figure 2a shows the storage modulus and loss modulus G' and G'' at the reference temperature of 100 °C. Figure 2b presents the WLF shift factor and parameters c_1 and c_2 at 100 °C in the WLF equation. Both the plateau modulus G_N^0 read from Figure 2a, i.e., G' at ω_{min} where $G''(\omega_{min}) = G''_{min}$, and that calculated according to $d^2G'(\omega)/d\omega^2 |_{\omega^*} = 0$, $G_N^0 = G'(\omega^*)$[18] give $G_N^0 = 0.675$ MPa. This result implies that the entanglement molecular weight M_e for this P(3HB-*co*-4HB) is around $M_e = \rho RT/G_N^0 = 4300$ g/mol, assuming a density of 0.9 g/cm^3 and $T = 373$ K.

For the semicrystalline samples such as sample A, the crystallization prevents us from applying tTs to probe the plateau region. Nevertheless, the oscillatory shear measurement is a useful tool to interrogate the crystallization temperature. Figure 2c shows the oscillatory shear data of sample A at temperatures between 100 and 130 °C in the frequency between 0.1 and 100

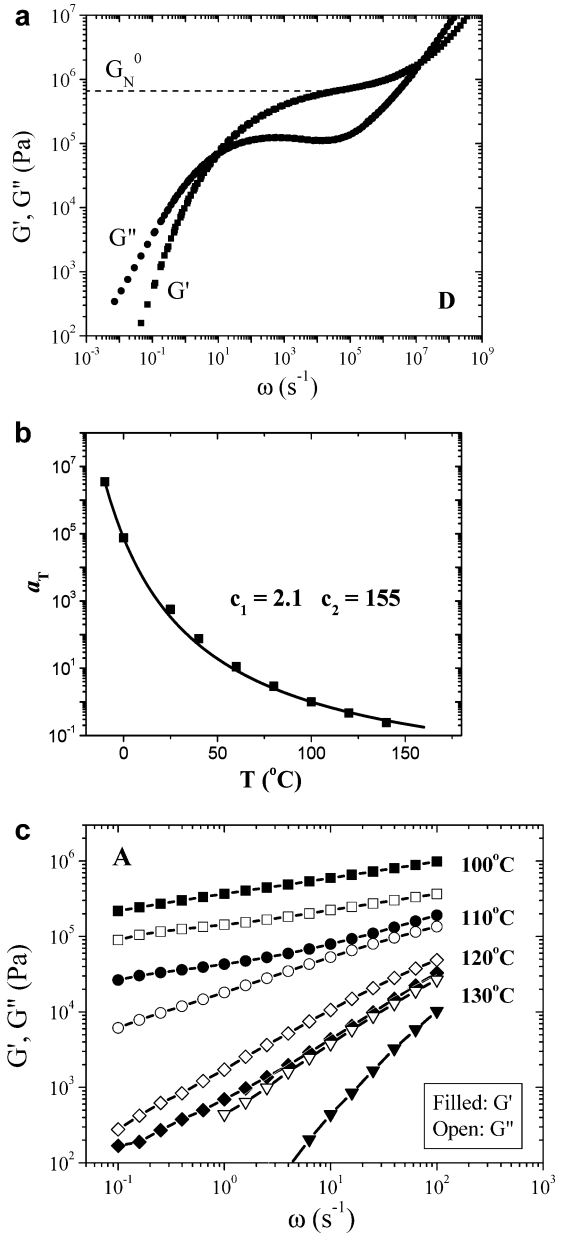

Figure 2. (a) Master curves for storage and loss moduli G' (in squares) and G'' (in circles) of sample D at a reference temperature of 100 °C. They were obtained by oscillatory shear measurements between −20 and 160 °C and using the time−temperature superposition. The plateau modulus, G_N^0, is determined to be 6.75×10^5 Pa. (b) The shift factor used to obtain the mater curves in (a), where the WLF parameters c_1 and c_2 are obtained by fitting to the WLF equation. (c) Oscillatory shear measurements of sample A at four different temperatures in the frequency range of 0.1−100 s^{-1}.

s^{-1}. Measurements at each temperature were from a separate sample loading. For measurements at 100 and 110 °C, the sample was first loaded at 120 °C to ensure a good contact between the sample and the two plates; the temperature was then lowered to 100 or 110 °C for 30 min before the measurement. For measurements at 120 and 130 °C, the sample was directly loaded at these temperatures. At temperatures of 100 and 110 °C, the storage modulus G' is higher than the loss modulus G'', implying a solid state at these temperatures. At temperature of 120 °C, G' is lower than G''. Nevertheless, G' and G'' curves are parallel to each other, indicating the existence of a "gel" state. At temperature of 130 °C, the G' curve and G'' curve have a crossing point, showing that the sample is in the terminal region and is a viscoelastic liquid. The melting temperature of sample A, as determined by the rheological characterization, is around 120 °C, which is some 30 °C higher than that indicated by DSC in Figure 1. This comparison indicates that the rheological signature for the presence of any crystallization is highly sensitive and consistent with the observed DSC behavior shown in Figure 1.

Capillary Flow Measurement. To provide information for processing design, capillary flow behavior was studied using a Monsanto capillary rheometer, equipped with a capillary die of $D = 1.12$ mm and $L/D = 20$. The measurement at each temperature was done with a separate sample loading. To avoid the possible thermal degradation, all the measurements were conducted at or below 160 °C, and for each loading the residue time of the materials staying in the barrel was controlled carefully within 20 min. Figure 3a−d shows the flow curves of samples A to D at temperatures between 90 and 160 °C, where the apparent wall shear rate $\dot{\gamma}$ is measured as a function of the applied shear stress σ. The flow curves of sample D, which has 31% 4HB, show a smooth change with the temperature. The flow curves of sample A show a strong separation between 110 and 120 °C, suggesting the melting transition is near 120 °C. The flow curves of sample B show a similar trend as sample A between 130 and 140 °C although less obvious. Sample C also displays a much reduced viscosity increase at 110 °C. A hint of a small amount of crystallization in sample C is consistent with the observed DSC measurement in Figure 1.

Finally, we examined the capillary flow characteristics of sample E. Because of the high viscosity of sample E, a capillary die of $D = 1.40$ mm and $L/D = 15$ was used, and flow curves were obtained only at 150 and 160 °C. At both temperatures a stick−slip transition was observed at around 0.30 MPa, and a periodic surface roughness (sharkskin) can be observed in the stress region between 0.10 and 0.30 MPa. The extrapolation length b can be used to quantify the magnitude of the stick−slip transition, which is related to the ratio of the apparent shear rates at the transition:[19]

$$\frac{\dot{\gamma}_{\text{slip}}}{\dot{\gamma}_{\text{stick}}} = 1 + \frac{8b}{D} \tag{1}$$

where D is the diameter of the capillary die. At 150 °C the value of b is measured to be 4.3 mm. We can also estimate b according to the formula[19] $b = (M/M_e)^3 a$, where a is a molecular length comparable to the tube diameter. If we take the original value for $M_w = 1022$K, $M_e = 4.3$K, and $a = 1$ nm, we slightly overestimate b, which implies that some degradation might have took place during the measurement.

The observed temperature dependence for samples A−D can be summarized in terms of the viscosity measurements at a given stress, as shown in Figure 4. It is important to note that the parallel lines in Figure 4 for all four samples in the molten state indicate approximately the same temperature dependence of the relaxation dynamics that govern the chain relaxation time and viscosity. In other words, the revealed WLF equation in Figure 2b is expected to describe the temperature dependence for all the samples above their melting points, and the activation energy is approxi-

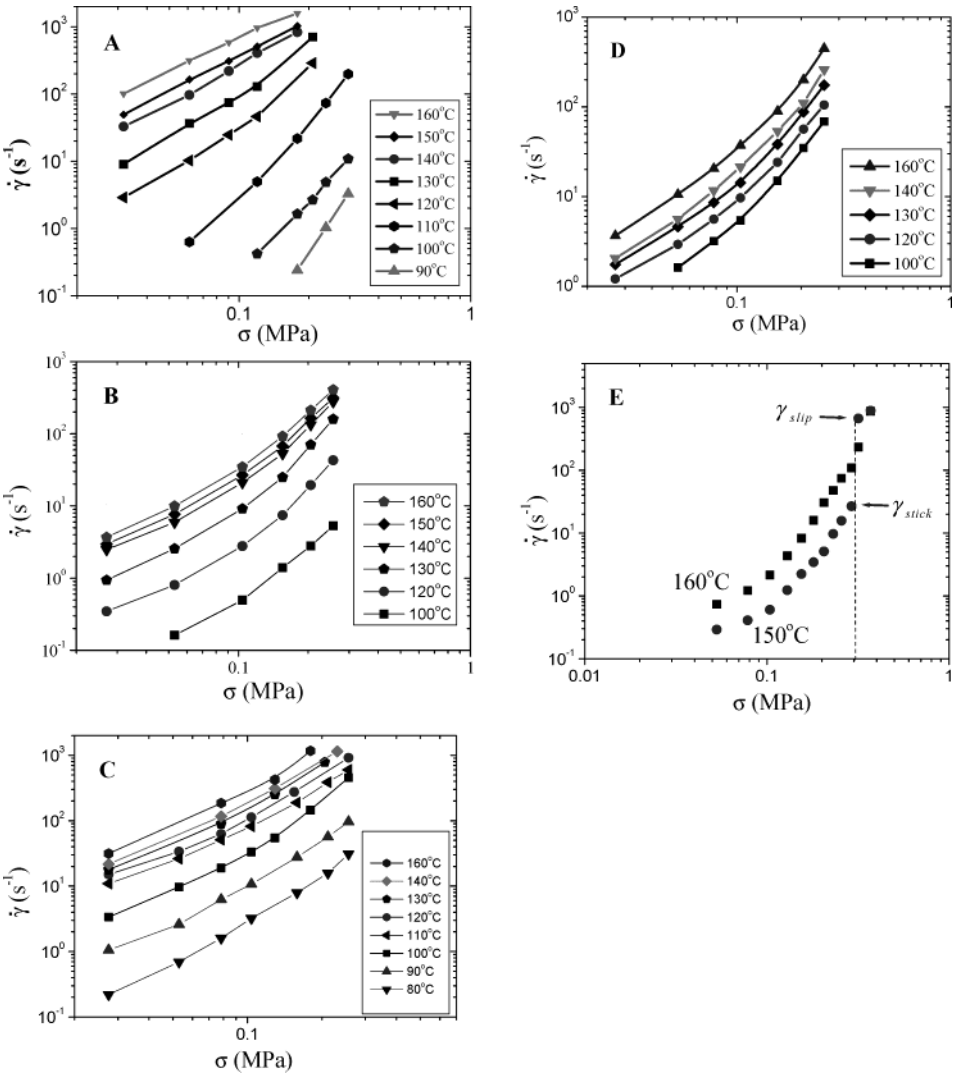

Figure 3. (a−e) Flow curves of samples A−E, respectively, at different temperatures obtained using the Monsanto capillary rheometer equipped with a capillary die of $D = 1.12$ mm and $L/D = 20$ (for A−D) or a capillary die of $D = 1.40$ mm and $L/D = 15$ (for E). The flow curve at each temperature was obtained from a separate sample loading.

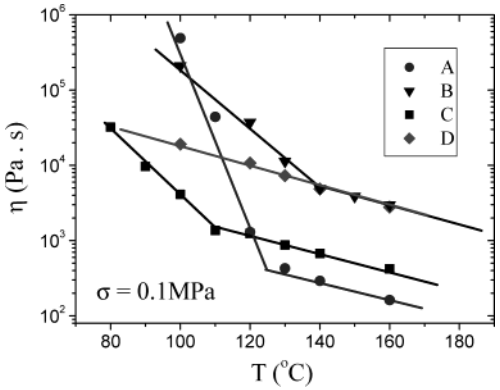

Figure 4. Steady flow viscosity of samples A−D at stress of 0.1 MPa as a function of temperature, calculated from Figure 3a−d.

mately independent of the 4HB content in the explored range. At lower temperatures, sample A's viscosity is observed to take off below 130 °C, sample B's viscosity increases strongly below 140 °C, and sample C's viscosity also deviates from its temperature dependence at higher temperatures at 110 °C. The sharp changes in the trend are indicative of presence of crystallization in these samples. Only sample D appears to be free of crystallization, a fact that is consistent with the DSC results.

It should be noted that despite a higher 4HB content in sample B and therefore a lower level of crystallinity according to the established correlation between 4HB content and crystallinity,[1] sample B appear to have its melting point at 140 °C, higher than that of sample A around 130 °C, confirming the DSC results in Figure 1. This implies that samples A and B may have some difference in the detailed crystallization morphology and structure, caused by the variations in the microbial synthesis processes.

The steady shear viscosity η of the five samples from A to E is evaluated at 160 °C and a shear stress σ equal to 0.1 MPa as a function of molecular weight, as shown in Figure 5. Similarly, η of the next five samples from F to J in Table 1 is measured at 150 °C and $\sigma = 0.2$ Pa. The shear thinning behavior causes the second group of data to stay below that of the first. All the samples have a similar molecular weight distribution of M_w/M_n around 2.0, allowing viscosity measurements at a fixed stress to reveal the scaling law expected from the standard reptation theory.[20]

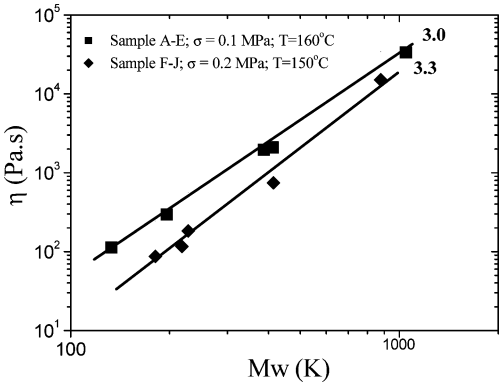

Figure 5. Steady shear viscosity of samples A−E at 160 °C and stress of 0.1 MPa as a function of molecular weight, calculated from Figure 3a−e.

Two comments are in order. The scaling exponent is lower than expected value of 3.4 perhaps because of a small amount of thermal degradation that these samples suffered during the measurements, which would have a greater impact for the samples of higher molecular weights. η for the samples from F to J displays the expected molecular weight scaling for entangled melts because they have all the same 4HB content. Since the scaling exponent is similar for the samples from A to E where the 4HB content varies, we infer that the entanglement molecular weight M_e is not strongly dependent on the 4HB content. This implies that the chain dynamic flexibility does not vary much with the 4HB content. In other words, the 4HB content only influences the melting temperature and the degree of crystallinity. Beyond the melting temperature, the 4HB content in P(3HB-*co*-4HB) copolymers does not affect the rheological properties, and the flow behavior is only determined by molecular weight and its contribution.

Creep Measurements (Controlled Stress). The creep behavior of P(3HB-*co*-4HB) copolymers was also investigated with a stress-controlled dynamic mechanical spectrometer (Bohlin) to characterize the crystallization and melting behavior rheologically. Similar to the procedure used in the oscillatory shear measurement in ARES, the samples were first loaded at 120 °C to ensure a good contact. After lowering the temperature to 90 °C for 30 min, the creep measurements were carried out in a sequence from low temperatures (90 °C) to high temperatures (160 °C) in an interval of 10 °C. At each temperature, the sample sits for 30 min before the measurement. For sample A at temperatures equal to or lower than 110 °C, a stress as high as 5000 Pa was applied due to its solidlike nature. For all other situations, a stress of 50 Pa was applied. Considering the dominant relaxation time τ for the amorphous sample D in the molten state is less than 0.1 s which can be read from Figure 2a, the creep time for all the measurements was chosen to be 100 s to ensure that the steady state is achieved in the molten state.

Figure 6a depicts the creep behavior of sample A in the temperature region between 90 and 160 °C, where the creep compliance at the fixed stresses was measured by Bohlin as a function of time. Here we have demonstrated perhaps for the first time how to use a controlled stress rheometer to characterize the melting behavior and to evaluate the crystallization effect on the rheological properties. Clearly, the melting took place upon heating the sample from 110 to 120 °C, where the sample turned from solidlike to liquidlike. In contrast,

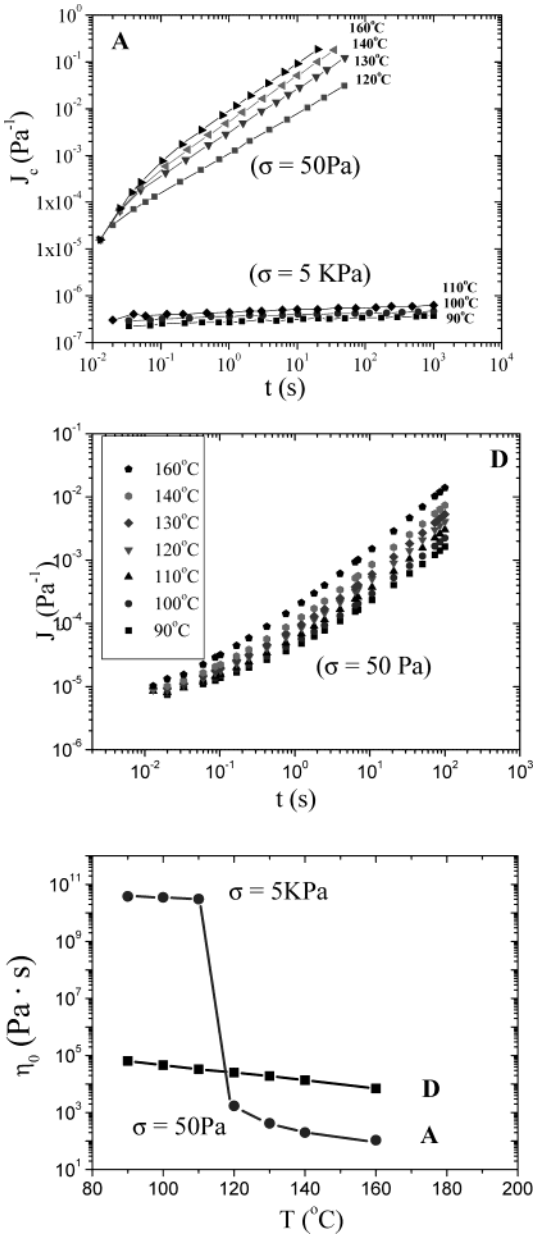

Figure 6. (a) Creep measurement of sample A at different temperatures from a stress-controlled parallel plate rheometer (Bohlin). The gap size is 1 mm. At the three lowest temperatures, because of the solid nature of the sample, a higher stress of 5 kPa was applied. (b) Similar creep measurement of sample D under a stress of 50 Pa as a function of temperature. (c) The low-shear viscosity of samples A and D calculated from (a) and (b) according to eq 2 as a function of temperature.

sample D shows, in Figure 6b, no abrupt change in its creep characteristics, which is consistent with the observed lack of crystallization as shown in Figures 1 and 4.

From the creep curves given in Figure 6a,b, a low-shear viscosity η_0 and equilibrium compliance J_e^0 can be calculated according to

$$J_c = J_e^0 + \frac{t}{\eta_0} \qquad (2)$$

where J_c is the steady-state compliance and t is the creep time.

The low-shear viscosity η_0 was found to change with temperature discontinuously for sample A and smoothly

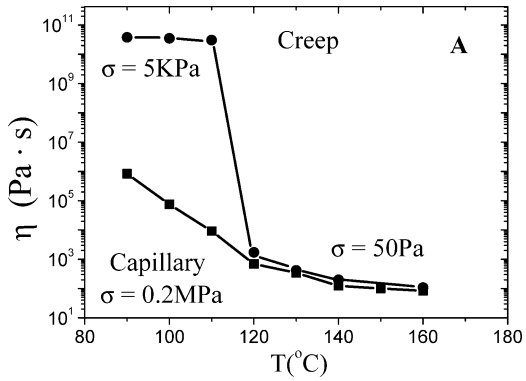

Figure 7. Comparison between the low-shear viscosity of sample A measured by creep and measured by capillary flow as a function of temperature. The data were obtained from Figure 6c and Figure 3a, respectively.

for sample D, as shown in Figure 6c. The sharp transition that occurs at 120 °C clearly indicates the melting point for sample A. By comparison, sample D is free of any crystallization in terms of its rheological characteristics.

The low-shear viscosity η_0 and the equilibrium compliance J_e^0 can also be calculated from the oscillatory shear master curve in terminal region according to[18]

$$\lim_{\omega \to 0} \frac{G''}{\omega} = \eta_0 \tag{3}$$

$$\lim_{\omega \to 0} \frac{G'}{\omega^2} = J_e^0 \eta_0^2 \tag{4}$$

For sample D at 100 °C, the calculation from the creep curve according to eq 2 and the calculation from the master curve according to eqs 3 and 4 both result in the low-shear viscosity η_0 of 4.6×10^4 Pa·s and the equilibrium compliance J_e^0 of 7.5×10^{-5} Pa^{-1}. The two methods give very close results, showing the consistency between the different measurements.

Figure 7 further compares the viscosity change of sample A upon crystallization as evaluated by both creep and capillary flow measurements. In the molten state, the two types of measurement agree well with each other. At lower temperatures, despite the crystallization, significant capillary flow was observed below T_m in contrast to the creep flow. This took place because the applied shear stress was apparently higher than a critical level, beyond which the sample yields, i.e., flows plastically.

Melting and Crystallization in a Thermal Cycle Characterized by Oscillatory Shear and DSC. The stress-controlled dynamic mechanical spectrometer (Bohlin) was also used to investigate the melting and crystallization behavior of P(3HB-*co*-4HB) in a heating and cooling thermal cycle. A disk sample of 1 mm thickness and 15 mm diameter was first loaded at 140 °C. Then the temperature was lowered at a rate of 2 °C/min until 80 °C, and the complex viscosity was recorded in this cooling process under a fixed stress of 100 Pa and frequency of 2 Hz. After 30 min at 80 °C, the sample was heated at a rate of 2 °C/min back to 140 °C, and the oscillatory shear response was again recorded under the same conditions. Figure 8 shows the complex viscosity of sample A in the heating and cooling ramp. Here the magnitude of η^* is smaller than η_0 of Figure 6c because the oscillation frequency of 2 Hz is much higher than the shear rate of less than 10^{-6} s^{-1}; i.e., the difference is due to the shear thinning.

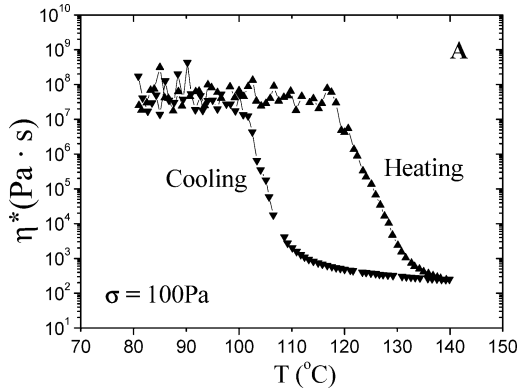

Figure 8. Oscillatory shear viscosity obtained from a stress-controlled parallel plate rheometer (Bohlin) in a cooling and heating cycle for sample A. The disk sample of 1 mm thickness and 15 mm diameter was first loaded at 140 °C. Then the temperature was lowered at a rate of 2 °C/min until 80 °C, and the complex viscosity was recorded in this cooling process under a fixed stress of 100 Pa and frequency of 2 Hz. After 30 min at 80 °C, the sample was heated at a rate of 2 °C/min back to 140 °C, and the oscillatory shear response was again recorded under the same conditions.

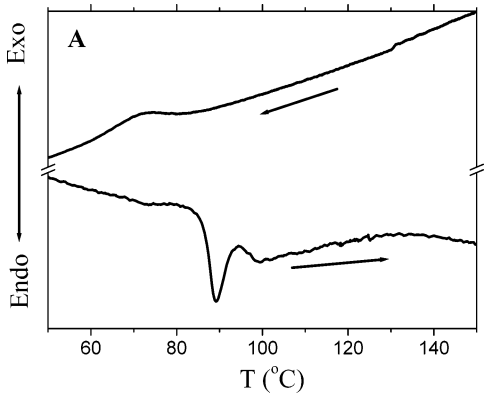

Figure 9. DSC curve of sample A from a heating and cooling thermal cycle. About 3−5 mg of sample A in the DSC pan was first heated from 50 to 160 °C at a rate of 2 °C/min; then after 2 min at 160 °C, the sample was cooled back to 50 °C at the same rate.

It is clear that the melting occurs at 120 °C during the heating ramp where the sample transferred from a solid state (high viscosity) to a liquid state (low viscosity). This is fully consistent with the creep measurement summarized in Figure 6c. On the other hand, the crystallization is more or less complete at 100 °C as far as its impact on rheology is concerned, 20 °C lower than the melting point. This result corroborates the earlier studies that supercooling is necessary for the crystallization process of PHA copolymers.[7]

As a comparison, a similar thermal cycle was also conducted in a DSC test, which is shown in Figure 9. About 3−5 mg of sample A held in the aluminum pan was first heated from 50 to 160 °C at a rate of 2 °C/min, then after stabilizing for 2 min, the sample was cooled back to 50 °C at the same rate. The endothermal curve was recorded. Figure 9 shows that the crystallization and melting points are 20 °C apart. It should also be noted that the melting peak in Figure 9 is narrower than that in Figure 1 due to the lower heating rate. The comparison between Figures 8 and 9 indicates that the rheological method is very sensitive to any

small amount of crystallization that is not detectable by DSC. As a result, the viscosity buildup occurs 30 °C lower than indicated by DSC.

Conclusion

The rheological properties of five P(3HB-*co*-4HB) copolymers have been systematically studied in pressure-driven capillary flow, oscillatory shear flow between parallel plates, and stress-controlled creep flow. It is established that the polymer with sufficiently high 4HB content is amorphous and obeys the time−temperature superposition. Its oscillatory shear behavior, along with its creep behavior, has allowed us to obtain an estimate of the entanglement molecular weight for the first time. Further capillary flow measurements of all the samples in their molten state have indicated that the variation in 4HB content does not significantly alter the value of M_e. Moreover, the viscosity of these samples appears to have nearly the same temperature dependence in their molten state, indicating the friction dynamics are essentially independent of the 4HB content in the explored temperature range. Crystallization occurs for the biopolyesters with lower 4HB contents. For the semicrystalline samples A, B, and C listed in Table 1, the melting and crystallization behavior affects the rheological properties significantly.

Therefore, we have applied the rheological methods based on creep and oscillatory shear measurements to characterize the crystallization and melting processes. In particular, we find using creep that the semicrystalline sample exhibits an abrupt rise in the steady shear viscosity upon reaching the crystallization temperature. Oscillatory shear measurements during a thermal cycle have been carried out to delineate the crystallization and melting characteristics in terms of a sharp viscosity buildup and decline around T_c and T_m, respectively. Thus, apart from the conventional way to detect crystallization by monitoring the behavior of storage and loss moduli G' and G'' in oscillatory shear, we have elucidated two more methods to characterize crystallization and evaluate its influence on the melt rheology: creep and capillary flow measurements both under controlled stress. In addition, oscillatory shear viscosity measurement appears to be a novel way to characterize crystallization and melting kinetics.

Acknowledgment. It is appropriate to acknowledge that Figure 2a was obtained by Shanfeng Wang in our lab. Goodyear's support for a summer internship (for Piwai Dakwa) is greatly appreciated. This work is supported, in part, by NSF CTS-0115867.

References and Notes

(1) Doi, Y. *Microbial Polyesters*; VCH Publishers Inc.: New York, 1990.
(2) Nakamura, S.; Doi, Y.; Scandola, M. *Macromolecules* **1992**, *25*, 4237.
(3) Ishida, K.; Wang, Y.; Inoue, Y. *Biomacromolecules* **2001**, *2*, 1285.
(4) Mitomo, H.; Hsieh, W. C.; Doi, Y. *Polymer* **2001**, *42*, 3455.
(5) Hori, Y.; Yamaguchi, A.; Hagiwara, T. *Polymer* **1995**, *36*, 4703.
(6) Kunioka, M.; Tamaki, A.; Doi, Y. *Macromolecules* **1989**, *22*, 694.
(7) Abe, H.; Doi, Y. *Macromol. Symp.* **2001**, *174*, 43.
(8) Mitomo, H.; Doi, Y. *Int. J. Biol. Macromol.* **1999**, *25*, 201.
(9) Kunioka, M.; Doi, Y. *Macromolecules* **1990**, *23*, 1933.
(10) Yoon, J. S.; Chin, I. J.; Kim, M. N.; Kim, C. *Macromolecules* **1996**, *29*, 3303.
(11) Doi, Y.; Kanesawa, Y.; Kunioka, M.; Saito, T. *Macromolecules* **1990**, *23*, 26.
(12) Scandola, M.; Ceccorulli, G.; Doi, Y. *Int. J. Biol. Macromol.* **1990**, *12*, 112−117.
(13) Spyros, A.; Marchessault, R. H. *Macromolecules* **1995**, *28*, 6108.
(14) Spyros, A.; Marchessault, R. H. *Macromolecules* **1996**, *29*, 2479.
(15) Choi, H. J.; Kim, J.; Jhon, M. S. *Polymer* **1999**, *40*, 4135.
(16) Choi, H. J.; Park, S. H.; Yoon, J. S.; Lee, H. S.; Choi, S. *J. Macromol. Sci.* **1995**, *A32*, 843.
(17) Choi, H. J.; Park, S. H.; Yoon, J. S.; Lee, H. S.; Choi, S. *J. Polym. Eng. Sci.* **1995**, *35*, 1636.
(18) Ferry, J. D. *Viscoelastic Properties of Polymers*; John Wiley & Sons: New York, 1980.
(19) Wang, S.-Q. *Adv. Polym. Sci.* **1999**, *138*, 227.
(20) Wang, S.-Q.; Drda, P. A. *Macromolecules* **1996**, *29*, 4115.

MA034219K